Biophysical *Journal*
Biophysical Letter

Biophysical Society

As a Nucleus Enters a Small Pore, Chromatin Stretches and Maintains Integrity, Even with DNA Breaks

Jerome Irianto,[1,2] Yuntao Xia,[1,2] Charlotte R. Pfeifer,[1,2,3] Roger A. Greenberg,[1,4] and Dennis E. Discher[1,2,3,*]
[1]Physical Sciences Oncology Center at Penn, [2]Molecular & Cell Biophysics Lab, [3]Graduate Group/Department of Physics & Astronomy, and [4]Cancer Biology, Abramson Family Cancer Research Institute, Perelman School of Medicine, University of Pennsylvania, Philadelphia, Pennsylvania

ABSTRACT As a cell pushes or pulls its nucleus through a small constriction, the chromatin must distort and somehow maintain genomic stability despite ever-present double-strand breaks in the DNA. Here we visualize within a living cell the pore-size dependent deformation of a specific locus engineered into chromosome-1 and cleaved. An mCherry-tagged nuclease targets the submicron locus, causing DNA cleavage and recruiting repair factors such as GFP-53BP1 to a large region around the locus. Aspiration of a cell and its nucleus into a micropipette shows that chromatin aligns and stretches parallel to the pore. Extension is largest in small pores, increasing >10-fold but remaining 30-fold shorter than the DNA contour length in the locus. Brochard and de Gennes' blob model for tube geometry fits the data, with a simple modification for chromatin crowding. Continuity of the highly extended, cleaved chromatin is also maintained, consistent with folding and cross bridging of the DNA. Surprisingly, extensional integrity is unaffected by an inhibitor of the DNA repair scaffold.

Cells have been seen to squeeze through small gaps of matrix and other cells in many basic processes that range from immune surveillance to disease, and include invasion of cancer cells into nearby tissue or entry into blood capillaries. The nucleus is the largest and stiffest organelle in the cell (1) but a cell can often push, pull, and forcibly distort this chromatin-filled organelle through a constriction (2,3). Pulling a flexible polymer into a tube is a classic problem in polymer physics (4), but any relevance to chromatin within a nucleus that is being pulled through a pore is unclear, particularly given the crowding estimated as ~70% chromatin volume fraction (5). Also unclear are the effects or not of double-strand breaks in the DNA backbone of chromatin, although such breaks—which seem to be present at low levels in all cells (6)—have been speculated to be enhanced by cell migration through small pores (2). When cleaved DNA is stretched by optical traps in single molecule studies, it is held together by a scaffold of repair factors (7), but chromatin is made up of many other cohesion-enhancing proteins, which motivates stretching of cleaved chromatin in intact nuclei of living cells.

A repetitive locus in one arm of chromosome-1 has been engineered previously into the U2OS osteosarcoma cell line for live cell imaging of the locus (8) (Fig. 1 *A*). The ~200 repeats of the lactose operon (LacO) add up to a DNA contour length >600 μm. In methanol-fixed cells, all of chromosome 1 can be seen by fluorescence in situ hybridization, revealing a fractal shape microns in size, indicative of chromatin folding (Fig. 1 *B*). In live cells, the locus can be seen by inducing expression of a fusion protein of lactose repressor (LacR)-mCherry-FokI nuclease. LacR binds to the LacO sequence, and FokI causes DNA breaks upon binding, based on accumulation of a DNA damage response protein, GFP-53BP1, at the locus and around it (Fig. 1 *C*). A histone that is modified upon DNA damage, γH2AX, also occupies the same large area as part of a repair scaffold complex (9,10). DNA cleavage by FokI nuclease is further supported by evidence of enhanced DNA synthesis at the locus, even though locus size appears unaffected by breaks and processes they activate (Fig. S1 in the Supporting Material).

The deformation dynamics of a specific chromosomal locus within an interphase nucleus have not been visualized previously, although the micromechanics of isolated mitotic chromosomes have been studied (11), as has the stretching of mitotic chromosomes in live yeast (12). To controllably deform and visualize the cleaved chromatin

Submitted July 1, 2016, and accepted for publication September 30, 2016.
*Correspondence: discher@seas.upenn.edu
Editor: Tamar Schlick.
http://dx.doi.org/10.1016/j.bpj.2016.09.047

Please cite this article in press as: Irianto et al., As a Nucleus Enters a Small Pore, Chromatin Stretches and Maintains Integrity, Even with DNA Breaks, Biophysical Journal (2016), http://dx.doi.org/10.1016/j.bpj.2016.09.047

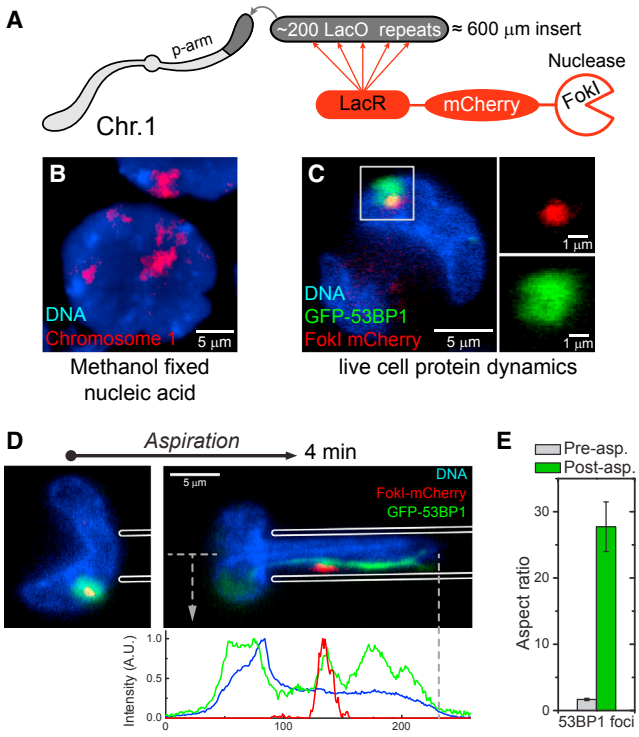

FIGURE 1 Chromosome-1 locus seen in live cells pulled into a micropipette. (*A*) The induced fusion protein has mCherry to visualize, LacR to bind LacO repeats in chromosome-1 DNA, and also FokI nuclease to cleave DNA in the locus. (*B*) Chr-1 as visualized by fluorescence in situ hybridization in fixed, dehydrated cells. (*C*) Colocalization of mCherry fusion protein with repair protein GFP-53BP1. (*D* and *E*) Within a nucleus in a micropipette, GFP-53BP1 extends and aligns, with an aspect ratio that increases >10-fold (n = 11 cells, N = 3 experiments).

within a living cell's nucleus, cells were detached from their substrate, their cytoskeleton was disassembled with latrunculin, and the intact cell was aspirated into a micropipette of diameter ~2.5–4.0 μm (13). Cells were studied within ~1 h of preparation. As the nucleus squeezes into the micropipette, the chromatin-bound GFP-53BP1 foci always align and stretch in the axial direction, increasing the aspect ratio >10-fold (Fig. 1 *D*). These observations begin to suggest that nuclear deformation affects chromatin organization.

The mCherry-labeled locus always stretches less than the repair scaffold of GFP-53BP1, but it also aligns as it enters the constriction (Fig. 2 *A*), adjacent to many other chromosomes pulled in parallel into the pore (i.e., blue DNA). The estimated diameter profiles of stretched FokI foci are close to the averages listed in Table S1, even though the profiles are calculated from just the initial width and the intensity profile (Fig. 2 *A*). A maximum stretched length of ~14 μm (Table S1) is <3% of the DNA contour length and thus indicates a high degree of chromatin folding. The foci stretch most upon entry and partially shorten as they displace further into the pore (Fig. S2). Convergent flow into such a constriction will stretch any small piece of fluid or solid material provided it is not overly compressible (Fig. S2). However, because the tube diameter remains constant after entry, the stretch should remain constant unless the material is more complex—as seems applicable here with recoil and reequilibration of the locus and the other chromatin in the pore.

The DNA damage response involves many factors, including ATM kinase that phosphorylates many targets (such as histone H2AX to produce γH2AX) in the recruitment of DNA repair proteins like 53BP1 (14). The ATM inhibitor KU55933, or ATMi, significantly attenuates γH2AX at the locus (Fig. S3) (15). Despite such attenuation of the repair scaffold, the mCherry foci stretch the same for ATMi treated cells and for not-treated cells—at least when comparing aspect ratio of foci aspirated into micropipettes of similar diameter (Fig. 2 *B*). Although the aspect ratios of stretched foci show no obvious correlations with either their original locations or their original sizes (Fig. S4), aspect ratios increase with decreasing pipette diameter. A statistically significant increase in

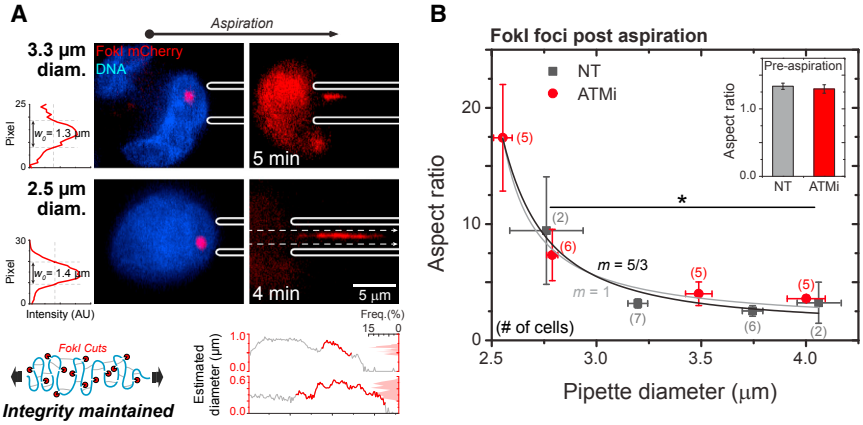

FIGURE 2 (*A*) FokI-mCherry focus also aligns and extends parallel to the pipette constriction. The diameter of preaspirated foci (w_0) at full width half-maximum was divided by the square-root of the cross-section intensity and multiplied by square-root of the intensity profile of stretched chromatin to calculate the diameter profile (*lower plots*). Integrity of chromatin is maintained. (*B*) Inhibition of DNA damage response by ATMi does not enhance FokI stretching. Data for ~2.8 and ~4 μm pipette diameter were pooled and show a significant change of aspect ratio with pipette diameter (*p = 0.05). (*Inset*) Aspect ratio of FokI foci before aspiration at ~1.3 μm (n = 17–21 cells, N > 3 experiments).

Please cite this article in press as: Irianto et al., As a Nucleus Enters a Small Pore, Chromatin Stretches and Maintains Integrity, Even with DNA Breaks, Biophysical Journal (2016), http://dx.doi.org/10.1016/j.bpj.2016.09.047

aspect ratio of foci also requires pore diameters smaller than ~3 μm.

A scaling picture first used to describe conformational changes of a single, self-avoiding chain confined to a tube or a pore (4,16) has been examined in simulations (17) and modified for soft walls (18). In simplest form, for a pore diameter d, the aspect ratio λ of a single chain is calculated from the parallel dimensions of the chain R_{par} divided by the perpendicular dimension R_{perp}, which gives $\lambda = R_{par} / R_{perp} \sim 1 / d^{5/3}$ when ignoring constant prefactors. The locus here is surrounded by chromatin so that the pore constricting the locus is much smaller than the pipette diameter, i.e., $d = (D_{pip} - c)$. Also, outside a pore ($D_{pip} \rightarrow \infty$), λ has the preaspiration aspect ratio ($a = 1.3$). Thus

$$\lambda = a + b/(D_{pip} - c)^m, \quad (1)$$

where $m = 5/3$ according to the blob theory. A good fit with $m = 5/3$ is achieved ($R^2 = 0.97$: $b = 2.9$, $c = 2.2$ μm), with other values of m also giving reasonable fits (Table S2). All data points (not-treated and ATMi) were fit because inhibition of the DNA damage response does not alter the trend in aspect ratio (i.e. nuclease dominates here).

Importantly, even though DNA within the engineered locus is constantly cleaved by nuclease, intensity profiles of mCherry indicate continuity so that integrity of the chromatin is maintained within a distended nucleus regardless of whether repair is inhibited (Fig. 2 *A*, *sketch*). Such locus integrity is consistent (in intact nuclei) with a highly folded structure being maintained by force-resistant chromatin cohesion factors (19).

In this Letter, we sought to show under native conditions of an interphase nucleus in a living cell that constriction-induced nuclear deformation orients and stretches a well-defined, cleaved chromatin locus parallel to the pore axis. Stretching is significant for a pore with a critical diameter <3 μm, but of course such a large pore is also constricting many nearby chromosomes within a crowded nucleoplasm. Potentially, chromatin compaction by small constrictions increases the volume fraction to a critical value, thus decreasing the accessible space within the nucleus (20) and, in turn, increasing the chromatin stretching. Importantly, the integrity of the stretched and cleaved locus is always maintained, which strongly indicates that constrictions are unlikely to provide sufficient stress to mechanically break the covalent bonds in both strands of DNA. Distortion and/or displacement of nuclease cleaved DNA could, however, disturb repair processes. This could be important because DNA misrepair can contribute to genomic instability, including insertions, deletions, or perhaps point mutations, all of which might contribute to cancer progression (21). For this reason and more, it is certainly worth clarifying what is happening within the multiple blobs of chromatin (Figs. 2 *A* and S2) that are caused by the extension of the single starting locus (Fig. 1 *C*).

SUPPORTING MATERIAL

Supporting Materials and Methods, four figures, and two tables are available at http://www.biophysj.org/biophysj/supplemental/S0006-3495(16)30881-5.

AUTHOR CONTRIBUTIONS

J.I., Y.X., and C.R.P. designed research, performed research, and analyzed data; R.A.G. contributed analytic tools; and D.E.D. analyzed data and wrote the article with J.I.

ACKNOWLEDGMENTS

The authors of this study were supported by the National Institutes of Health, National Cancer Institute award U54 CA193417 and National Heart, Lung, and Blood Institute award R21-HL128187. The content is solely the responsibility of the authors, and does not necessarily represent official views of the National Institutes of Health.

REFERENCES

1. Dahl, K. N., P. Scaffidi, …, T. Misteli. 2006. Distinct structural and mechanical properties of the nuclear lamina in Hutchinson-Gilford progeria syndrome. *Proc. Natl. Acad. Sci. USA.* 103:10271–10276.
2. Harada, T., J. Swift, …, D. E. Discher. 2014. Nuclear lamin stiffness is a barrier to 3D migration, but softness can limit survival. *J. Cell Biol.* 204:669–682.
3. Wolf, K., M. Te Lindert, …, P. Friedl. 2013. Physical limits of cell migration: control by ECM space and nuclear deformation and tuning by proteolysis and traction force. *J. Cell Biol.* 201:1069–1084.
4. Brochard, F., and P. G. Degennes. 1977. Dynamics of confined polymer chains. *J. Chem. Phys.* 67:52–56.
5. Bancaud, A., S. Huet, …, J. Ellenberg. 2009. Molecular crowding affects diffusion and binding of nuclear proteins in heterochromatin and reveals the fractal organization of chromatin. *EMBO J.* 28:3785–3798.
6. Saul, R. L., and B. N. Ames. 1986. Background levels of DNA damage in the population. *Basic Life Sci.* 38:529–535.
7. Brouwer, I., G. Sitters, …, G. J. Wuite. 2016. Sliding sleeves of XRCC4-XLF bridge DNA and connect fragments of broken DNA. *Nature.* 535:566–569.
8. Shanbhag, N. M., I. U. Rafalska-Metcalf, …, R. A. Greenberg. 2010. ATM-dependent chromatin changes silence transcription in *cis* to DNA double-strand breaks. *Cell.* 141:970–981.
9. Rogakou, E. P., C. Boon, …, W. M. Bonner. 1999. Megabase chromatin domains involved in DNA double-strand breaks in vivo. *J. Cell Biol.* 146:905–916.
10. Schultz, L. B., N. H. Chehab, …, T. D. Halazonetis. 2000. p53 binding protein 1 (53BP1) is an early participant in the cellular response to DNA double-strand breaks. *J. Cell Biol.* 151:1381–1390.
11. Marko, J. F. 2008. Micromechanical studies of mitotic chromosomes. *Chromosome Res.* 16:469–497.
12. Fisher, J. K., M. Ballenger, …, K. Bloom. 2009. DNA relaxation dynamics as a probe for the intracellular environment. *Proc. Natl. Acad. Sci. USA.* 106:9250–9255.
13. Pajerowski, J. D., K. N. Dahl, …, D. E. Discher. 2007. Physical plasticity of the nucleus in stem cell differentiation. *Proc. Natl. Acad. Sci. USA.* 104:15619–15624.

Please cite this article in press as: Irianto et al., As a Nucleus Enters a Small Pore, Chromatin Stretches and Maintains Integrity, Even with DNA Breaks, Biophysical Journal (2016), http://dx.doi.org/10.1016/j.bpj.2016.09.047

14. Ward, I. M., K. Minn, …, J. Chen. 2003. Accumulation of checkpoint protein 53BP1 at DNA breaks involves its binding to phosphorylated histone H2AX. *J. Biol. Chem.* 278:19579–19582.

15. Hickson, I., Y. Zhao, …, G. C. Smith. 2004. Identification and characterization of a novel and specific inhibitor of the ataxia-telangiectasia mutated kinase ATM. *Cancer Res.* 64:9152–9159.

16. Daoud, M., and J. P. Cotton. 1982. Star-shaped polymers—a model for the conformation and its concentration-dependence. *J. Phys.* (*Paris*). 43:531–538.

17. Kalb, J., and B. Chakraborty. 2009. Single polymer confinement in a tube: correlation between structure and dynamics. *J. Chem. Phys.* 130:025103.

18. Morrison, G., and D. Thirumalai. 2005. The shape of a flexible polymer in a cylindrical pore. *J. Chem. Phys.* 122:194907.

19. Sun, M., T. Nishino, and J. F. Marko. 2013. The SMC1-SMC3 cohesin heterodimer structures DNA through supercoiling-dependent loop formation. *Nucleic Acids Res.* 41:6149–6160.

20. Kang, H., Y. G. Yoon, …, C. Hyeon. 2015. Confinement-induced glassy dynamics in a model for chromosome organization. *Phys. Rev. Lett.* 115:198102.

21. Jackson, S. P., and J. Bartek. 2009. The DNA-damage response in human biology and disease. *Nature.* 461:1071–1078.

Biophysical Journal, Volume *112*

Supplemental Information

As a Nucleus Enters a Small Pore, Chromatin Stretches and Maintains Integrity, Even with DNA Breaks

Jerome Irianto, Yuntao Xia, Charlotte R. Pfeifer, Roger A. Greenberg, and Dennis E. Discher

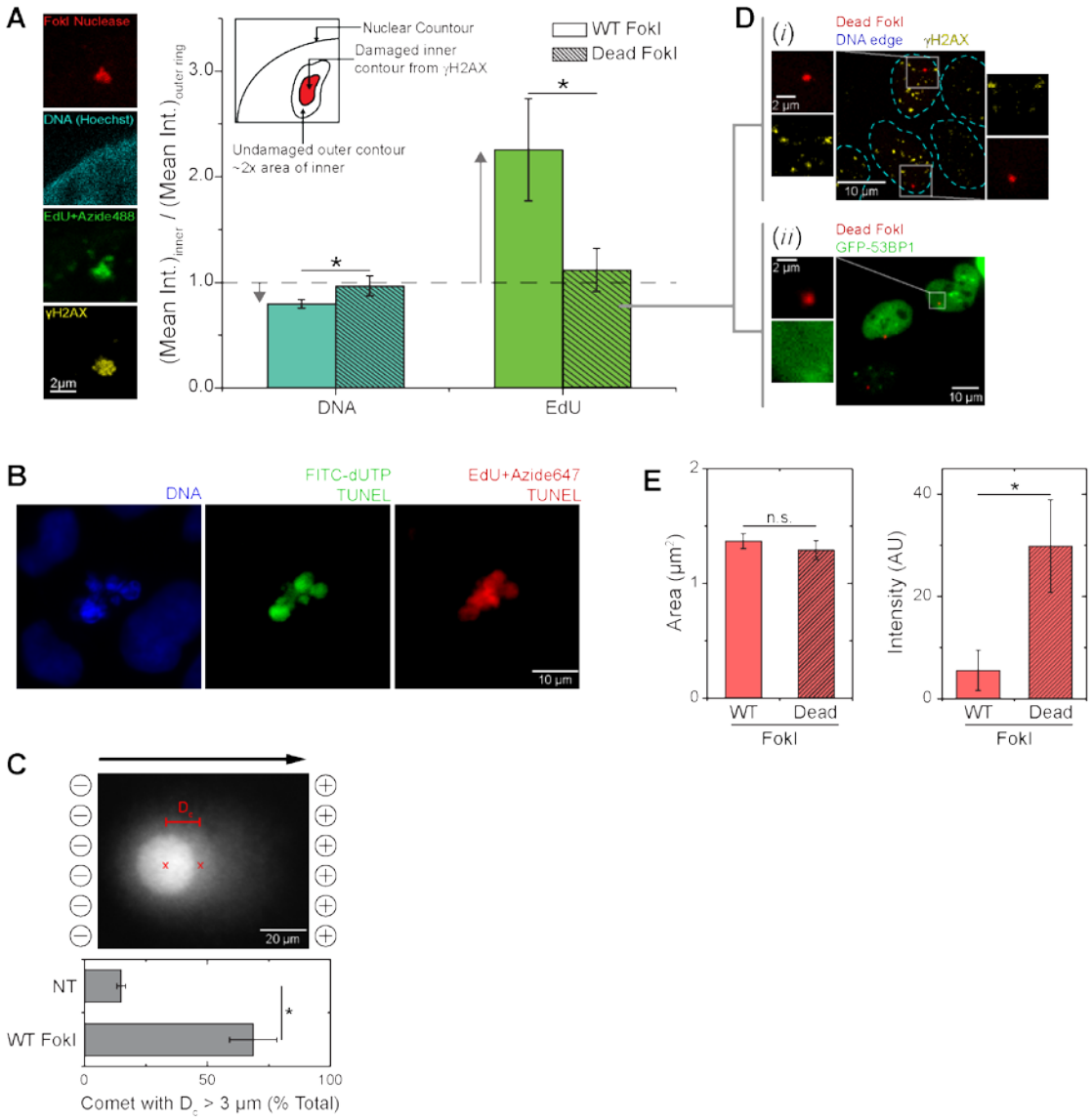

Figure S1 DNA damage at the wild-type (WT) FokI focus was confirmed by accumulation of EdU and DNA damage response (DDR) proteins as well as by comet assay, whereas dead FokI foci (D540A mutant) shows no EdU or DDR. **(A)** EdU was added to FokI-activated cells, where it accumulated at the FokI-damaged locus, as did DDR protein γH2AX. Comparing the mean intensity of the locus to that of the surrounding area reveals enrichment of EdU and depletion of DNA in the presence of WT—but not dead—FokI (>12 cells per group, n≥ 3 experiments, *$p < 0.05$). **(B)** Representative image of a TUNEL-positive and fixed apoptosing cell confirms that EdU is incorporated into damaged DNA by the transferase added for TUNEL assays. **(C)** Upon activation of WT FokI, a higher proportion of cells show a centroid shift (D_c) greater than 3 μm, which confirms by comet assay the presence of elevated DNA damage (>150 cells per group, n = 3 experiments, *$p < 0.05$). **(D)** Over-expression of dead FokI leads to accumulation of mCherry signal at the LacO locus. However, in contrast to WT FokI foci, dead FokI foci do not recruit DDR proteins γH2AX ***(i)*** nor GFP-53BP1 ***(ii)***. **(E)** The sizes of WT and dead FokI foci are very similar, but the intensity of WT FokI foci is much lower, which could indicate cleavage of DNA binding sites by WT FokI (>10 cells per group, n ≥ 3 experiments, *$p < 0.05$).

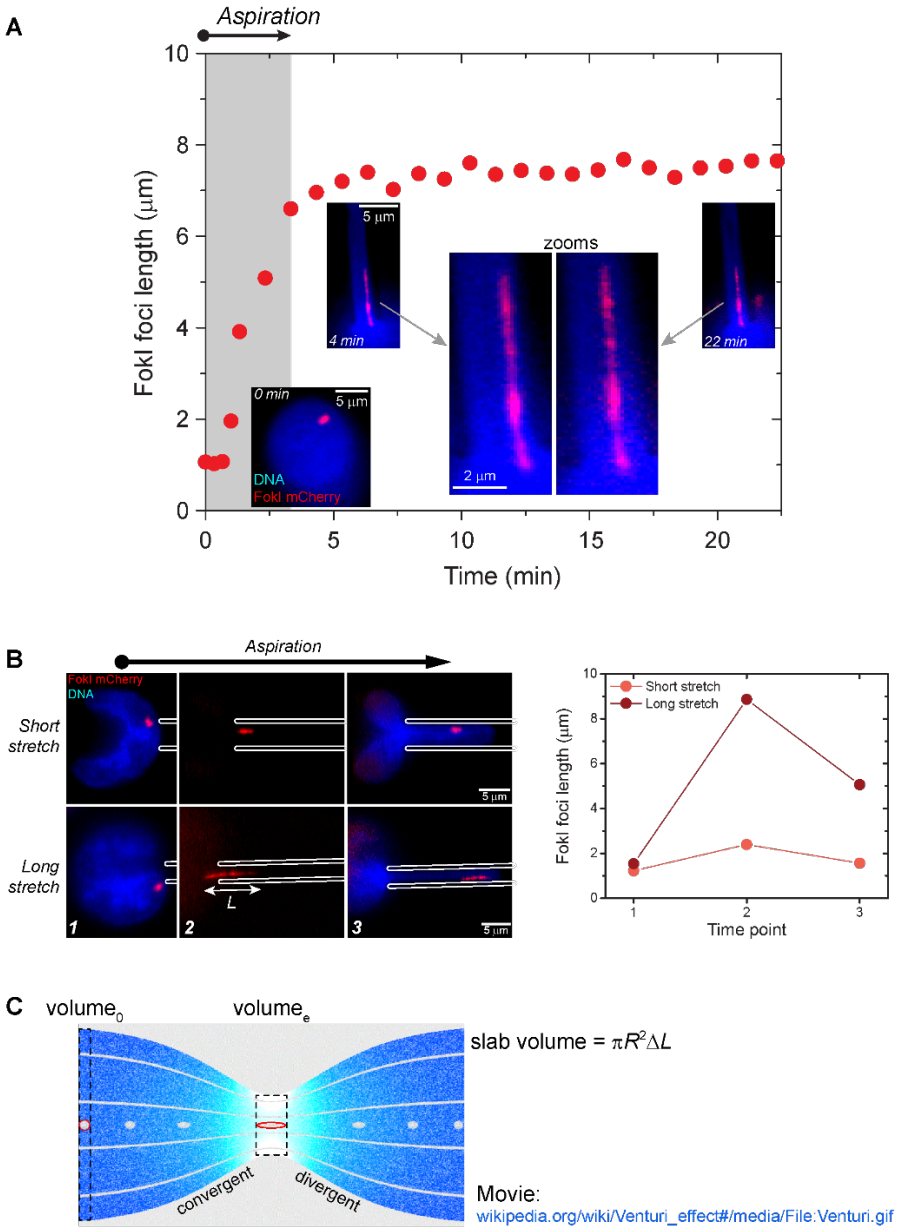

Figure S2 (A) FokI focus stretch as it enters pipette constriction. If we stop the aspiration and hold the foci in place, the length stay relatively constant over time (held for ~20 minutes). **(B)** A FokI focus stretches most at the pipette entrance, and then relaxes as it travels through the constriction. (Left) Representative images show a shorter and a longer FokI focus during aspiration. Both of them relax afterwards, but evidence of the former stretching is more obvious in the longer focus. (Right) Quantification of FokI foci length of the representative images. Mass conservation for a thin slab of material outside the pore (of area ~ R_o^2, velocity $\Delta L_o/\Delta t$), where the locus is unstretched, that then displaces into the pore (area ~ R_e^2, velocity $\Delta L_e/\Delta t$), where the locus is unstretched, can be expressed as $R_o^2\ \Delta L_o/\Delta t = R_e^2\ \Delta L_e/\Delta t$. The approximate elongation would be $\Delta L_e/\Delta L_o = (R_o/R_e)^2 > 1$, although any density change would alter this estimate, and lateral shrinkage makes the aspect ratio = $(R_o/R_e)^3$. Past the entry into the same micropipette, there should be no further change in elongation or aspect ratio

unless the chromatin within somehow relaxes and re-equilibrates, which clearly occurs. **(C)** Illustration of deformation induced in convergent flow.

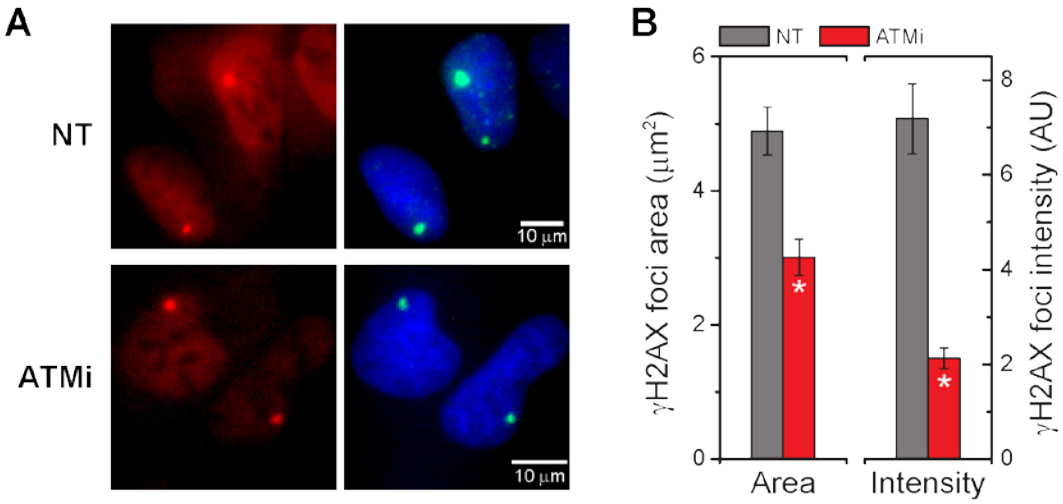

Figure S3 Inhibition of DNA damage response by ATMi reduces the FokI-induced gH2AX area and intensity. **(A)** Representative images show the reduction of gH2AX at the corresponding FokI foci. (B) Quantification of FokI-correlated gH2AX foci shows that ATMi reducse both gH2AX focus area and intensity (n = 52-57 nuclei per group*p<0.001).

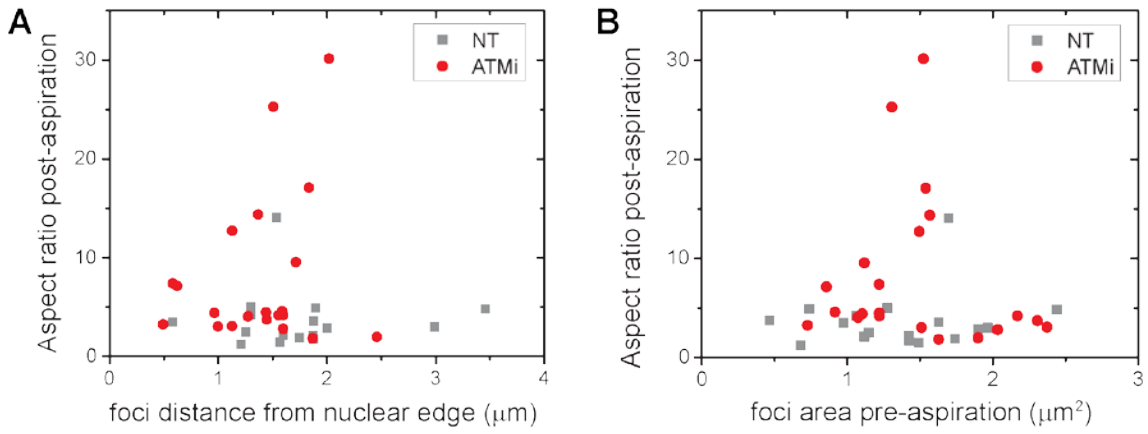

Figure S4 FokI focus aspect ratio post-aspiration does not correlate with focus distance from the nuclear edge pre-aspiration **(A)** nor with focus area pre-aspiration **(B)**.

Table S1 FokI foci maximum length and width during micropipette aspiration

Sample name	Post-aspiration	
	FokI foci length (µm)	**FokI foci width (µm)**
NT 1	1.13	0.91
NT 2	1.37	0.93
NT 3	1.40	0.67
NT 4	1.48	0.87
NT 5	1.51	0.60
NT 6	1.69	0.78
NT 7	2.03	0.58
NT 8	2.26	0.45
NT 9	2.29	1.21
NT 10	2.30	0.61
NT 11	2.37	0.48
NT 12	2.47	0.83
NT 13	2.53	0.88
NT 14	2.53	0.60
NT 15	2.80	0.78
NT 16	3.34	0.69
NT 17	8.09	0.58
ATMi 1	1.78	0.55
ATMi 2	1.81	0.99
ATMi 3	2.02	0.67
ATMi 4	2.02	0.45
ATMi 5	2.05	0.67
ATMi 6	2.13	0.48
ATMi 7	2.17	0.52
ATMi 8	2.22	0.55
ATMi 9	2.43	0.87
ATMi 10	2.48	1.26
ATMi 11	2.62	0.57
ATMi 12	2.86	0.68
ATMi 13	2.91	0.78
ATMi 14	3.89	0.55
ATMi 15	4.44	0.60
ATMi 16	4.61	0.48
ATMi 17	6.51	0.45
ATMi 18	6.64	0.52
ATMi 19	7.72	0.45
ATMi 20	10.20	0.40

ATMi 21	14.54	0.48

Table S2. Goodness of fit and other parameters predicted by the blob model in Eq.1, fitted on data in Fig. 2A, by using various values of m

m	R^2	b	c
0.5	0.94	3	2.5 µm
1	0.97	2.6	2.4 µm
2	0.97	3.5	2.1 µm
3	0.96	7.7	1.8 µm

Materials and methods

Cell culture U2OS human osteosarcoma cells were cultured in DMEM high glucose media (Gibco, Life Technologies) supplemented with 10% FBS and 1% penicillin/streptomycin (Sigma-Aldrich). Two-hundred fifty-six lac operator repeats (~9kb each) were integrated into the p-end of chromosome 1 of the U2OS cells used in this study. DNA damage at this site was induced by 3-to-6-hour incubation in 4-hydroxytamoxifen (Sigma) and Shield1 ligand (Clontech) [S1], which together activate the endonuclease FokI-mCherry-lac repressor construct. To over-express GFP-53BP1 and LacR-mCherry-D450A FokI (dead FokI), cells were transfected with Lipofectamine 2000 (Invitrogen, Life Technologies) for 24 hours prior to further experimentation. The DNA damage response was inhibited by a 10 μM ATM inhibitor, KU55933 (ATMi, Abcam), that was introduced to the cells an hour prior to FokI activation.

Immunostaining and imaging Cells were fixed in 4% paraformaldehyde (Sigma) for 15 minutes, followed with 10 minutes permeabilization by 0.5% Triton-X (Sigma), 30 minutes blocking by 5% BSA (Sigma), overnight incubation in primary antibody for γH2AX (Milipore), 1.5 hours incubation in secondary antibodies (ThermoFisher) and their nuclei were stained with 8 μM Hoechst 33342 (ThermoFisher) for 15 minutes. Epifluorescence imaging was done using an Olympus IX71—with a 40×/0.6 NA or 60×/1.2 NA objective—and a digital sCMOS camera (Prime 4.2, Photometrics). Confocal imaging was done on a Leica TCS SP8 system, equipped with a 63×/1.4 NA oil-immersion objective. ImageJ [S2] and MATLAB were used to quantify the resulting images.

Fluorescence in situ hybridization (FISH) Cells were detached with Trypsin-EDTA, and then underwent sample preparation and probe hybridization per manufacture's recommended protocol (Creative bioarray). Samples were imaged using an epifluorescence microscope with a 150x/1.45 NA.

EdU labeling and staining EdU (10 μM, Abcam) was added to U2OS culture 3 hours before fixation and permeabilization as described. Then, samples were stained with 100 mM Tris (pH 8.5), 1 mM $CuSO_4$, 100 μM azide dye (488 or 647) and 100 mM ascorbic acid (all from sigma) for 30 min at room temperature. After thoroughly washed, samples underwent immunostaining as described above.

TUNEL and Comet assay U2OS cells were fixed and permeabilized as described above and subjected to TUNEL assay per manufacturer's protocol (Roche), EdU was also added to the TUNEL

reaction and stained per description above. Alkaline comet assays were performed according to the manufacturer-issued protocol (Cell Biolabs).

Micropipette aspiration Prior to aspiration experiments, cells were detached with Trypsin-EDTA and treated with 0.2 μg/mL latrunculin-A (Sigma) for 1 hour at 37^{o}C, as described previously [S3], before being re-suspended in aspiration buffer (PBS with 1% BSA). Nuclei were stained with 8 μM Hoechst 33342 for 15 minutes. Epifluorescence imaging was done using a Nikon TE300, with a digital EMCCD camera (512B, Photometrics) and a 60x/1.25 oil-immersion objective. Image quantification and processing were performed in ImageJ [S2].

References

S1. Shanbhag, N. M., I. U. Rafalska-Metcalf, C. Balane-Bolivar, S. M. Janicki, and R. A. Greenberg, ATM-dependent chromatin changes silence transcription in cis to DNA double-strand breaks. ***Cell***. 141 (6):970-81, 2010.

S2. Schneider, C. A., W. S. Rasband, and K. W. Eliceiri, NIH Image to ImageJ: 25 years of image analysis. ***Nat Methods***. 9 (7):671-5, 2012.

S3. Pajerowski, J. D., K. N. Dahl, F. L. Zhong, P. J. Sammak, and D. E. Discher, Physical plasticity of the nucleus in stem cell differentiation. ***PNAS***. 104 (40):15619-24, 2007.